

Accepted Manuscript

Densification behaviour in forming of sintered iron-0.35% carbon powder metallurgy preform during cold upsetting

S. Narayan, A. Rajeshkannan

PII: S0261-3069(10)00485-1
DOI: [10.1016/j.matdes.2010.08.010](https://doi.org/10.1016/j.matdes.2010.08.010)
Reference: JMAD 3268

To appear in: *Materials and Design*

Received Date: 17 May 2010
Accepted Date: 8 August 2010

Please cite this article as: Narayan, S., Rajeshkannan, A., Densification behaviour in forming of sintered iron-0.35% carbon powder metallurgy preform during cold upsetting, *Materials and Design* (2010), doi: [10.1016/j.matdes.2010.08.010](https://doi.org/10.1016/j.matdes.2010.08.010)

This is a PDF file of an unedited manuscript that has been accepted for publication. As a service to our customers we are providing this early version of the manuscript. The manuscript will undergo copyediting, typesetting, and review of the resulting proof before it is published in its final form. Please note that during the production process errors may be discovered which could affect the content, and all legal disclaimers that apply to the journal pertain.



**DENSIFICATION BEHAVIOUR IN FORMING OF SINTERED IRON-0.35%
CARBON POWDER METALLURGY PREFORM DURING COLD
UPSETTING**

S. Narayan^a, A. Rajeshkannan^{b,*}

Co-Author

^aMr. SUMESH NARAYAN

Assistant Lecturer, Mechanical Engineering,
School of Engineering and Physics,
Faculty of Science, Technology & Environment,
The University of the South Pacific, Laucala Campus,
PO Box 1168, Suva, FIJI.
Off. No. +679 3232034,
Fax No. +679 3231538,
Email: narayan_su@usp.ac.fj

*** Corresponding Author**

^bDr. A. RAJESH KANNAN

Lecturer, Mechanical Engineering,
School of Engineering and Physics,
Faculty of Science, Technology & Environment,
The University of the South Pacific, Laucala Campus,
PO Box 1168, Suva, FIJI.
Off. No. +679 3232695,
Fax No. +679 3231538,
Email: ananthanarayanan_r@usp.ac.fj

Abstract

Plastic deformation is an important process to improve and obtain final product for sintered powder materials to compete with solid metal formed parts. The densification behaviour and forming limits of sintered iron-0.35% carbon steel preforms with different aspect ratios, during cold upsetting with two different lubricating constraints namely nil/no and graphite lubricant were investigated experimentally and is presented in this work. Powder preforms having initial theoretical density value of 84%, with two different aspect ratios were prepared using a suitable die-set assembly on a 1 MN capacity hydraulic press. Sintering operation was carried in an electric muffle furnace at the temperature of 1200⁰C for a holding period of 1.5 hours. Each sintered compact was subjected to incremental compressive loading of 0.05 MN under two different lubricant conditions till a visible crack appeared at the free surface. The densification mechanism is developed by studying the behaviour of densification against induced strain and Poisson's ratio. Further, attained density is considered to establish flow stress and formability stress index behaviour. Increased frictional constraints produces high circumferential stress on the free surface due to barreling effect and hence inhibits forming limits. The present work provides a guideline for producing P/M components free from open surface pores.

Keywords: Powder metallurgy C; Failure analysis H; Plastic behaviour F.

Nomenclature

C	Carbon
Fe	Iron
ε_{θ}	True hoop strain
ε_z	True axial strain
J_1	First invariant of the stress tensor
J_2'	Second invariant of the stress deviator
Y_0	Yield strength of a solid material, Pa.
Y	Yield strength of a partially dense material, Pa.
ρ	Fractional theoretical density
ρ_0	Initial fractional theoretical density
σ_z	Axial stress, Pa
σ_{θ}	Hoop stress, Pa
σ_r	Radial stress, Pa
σ_m	Hydrostatic stress, Pa
σ_{eff}	Effective stress, Pa
β	Stress formability factor

1. Introduction

Powder forging have been studied extensively and raising much interest in many parts of the industry as economic method of producing high strength, high ductility parts from metal powders [1] as powder metallurgy (P/M) method competes with other methods on the basis of cost which can be lower for high volume production of complicated components. The P/M technology is conducive nearly any material that can be processed in powder form. This technology is sometimes the only manufacturing method used to produce parts using materials such as porous materials, composite materials, refractory materials and special high duty alloys [2]. The vast application of ferrous powder metallurgy material in automotive and aerospace industry provides reasons for researchers to analyze powder metallurgy materials behaviour under metal forming processes [3]. Sintered P/M compacts are made by the process of compacting and sintering ferrous powder and non-metal powder. A known limitation of this route is the large number of small voids left in components after sintering. Plastic deformation is a main way to improve the performance of sintered ferrous material and obtain the final product. In general the preform produced by the conventional process will undergo so large degree of plastic deformation with enhanced level of densification [4,5]. Though plastic deformations of powder preforms is similar to that of conventional fully dense material, the additional complications are because of substantial amount of void fractions. Because there is a large number of residual porosity in the sintered powder materials, plastic volume change of sintered compacts will result from the void reducing and closing during plastic deformation. During the elastic deformation of fully dense material, Poisson's ratio remains constant and it is a property of the material; this ratio being 0.5 for all materials that conform to volume constancy. However, in the plastic deformation of

sintered P/M preforms, density changes occur, resulting in Poisson's ratio remaining less than 0.5 and tending to approach 0.5 only in the near vicinity of the theoretical density. Since the primary cause of fracture in upsetting is the circumferential tensile stresses, it is therefore essential to investigate fracture during cold upsetting of sintered powder materials [5-7].

It has been reported [8,9] that powder metallurgy route processing involves one die and one deformation stroke hence proper die design, processes and external constraints so as to produce components free from open surface pores must be determined. Sintered P/M preforms are particularly prone to fracture during forging because the presence of high amounts of pores in the preform act as stress risers hence lubrication also influences metal flow in a generally beneficial manner with respect to crack formation. Lubrication is important in most metal forming processes particularly in cold metal forming because good lubrication improves the quality of products through the reduction of defects and improvement in the dimensional accuracy and surface finish [9-11]. Investigation has shown that the increase of friction condition at die contact surface during deformation substantially increases the stresses. The exact shape is obtained from a final forging process, however, voids in sintered compacts exert a damaging effect on mechanical properties, and fracture may occur in workpiece as a result of major deformation in the forging process. The forming limit of porous preforms is a matter of great concern and the workability of metals is an important parameter in designing of forming operation [12,13].

The important parameters controlling the metal flow during the upset forging are the preform shape, dimensions and density and it is well understood that increasing the

density of the P/M parts is the best way to increase the performance of these parts, however, the essential governing factor for such design is found to be that the final product must be free from defects such as cracks [14,15]. Thus, present investigation is aimed to investigate and to establish the technical relationship that exists between the resistance to deformation against induced height strain and the attained densification as well as to evaluate the effect of die lubricant conditions during cold deformation of sintered Fe-0.35%C preforms of constant theoretical density and two different lubricating constraints with two different initial aspect ratios.

2. Experimental details

2.1 Materials and characterization

Atomized iron powder of less than or equal to 150 μm size and graphite powder of 2-3 μm size were used in the present investigation. Analysis indicated that the purity of iron was 99.7 percent and the rest were insoluble impurities. The characteristic of iron powder and Fe-0.35%C blend are shown in Table 1 and 2.

Table 1. Characterization of iron powder and Fe-0.35%C blend

Table 2. Sieve size analysis of iron powder

2.2 Blending, compaction and sintering

A powder mix corresponding to the aforementioned system was taken in a stainless steel pot with the powder mixed to porcelain balls (10 mm – 15 mm diameter) with a ratio of 1:1 by weight. The pot containing the blended powder was subjected to the blending operation by securely tightening and then fixing it to the pot mill. The mill was operated for 20 hours to obtain a homogenous mix. Green compacts of 26 mm diameter with 9 mm and 16 mm of length were prepared. The powder blend was

compacted on a 1.0 MN hydraulic press using a suitable die, a punch and a bottom insert in the pressure range of 430 ± 10 MPa to obtain an initial theoretical density of 0.84 ± 0.01 . In order to avoid oxidation during sintering and cooling, the entire surface of the compacts were indigenously formed ceramic coated. These ceramic coated compacts were heated in the electric muffle furnace with temperature of $1200^{\circ}\text{C} \pm 10^{\circ}\text{C}$. At this temperature the compacts were sintered for 90 minutes followed by furnace cooling.

2.3 Cold deformation

Sintered and furnace cooled preforms were machined to such a dimension so as to provide height-to-diameter ratio of 0.40 and 0.6 respectively. The initial dimensions of the cylindrical preforms were measure and recorded and used to calculate the initial density. Each specimen was compressively deformed between a flat die-set in the incremental loading step of 0.05 MN using 1 MN capacity hydraulic press under friction conditions, which included dry, unlubricated dies called nil/no lubricant condition and lubrication consisting of graphite paste (i.e. graphite with acetone) called graphite lubricant condition. The deformation process was stopped once a visible crack appeared at the free surface. Dimensional measurements such as deformed height, deformed diameters (including bulged and contact) were carried out after every step of deformation using digital vernier caliper and the density measurements being carried out using the Archimedes principle. Experimental results were used to calculate the flow stress, true height strain, true diameter strain, percentage theoretical density and Poisson's ratio.

3. Theoretical analysis

A typical theorem is that the plastic deformation occurs when the elasticity strain energy reaches a critical value. The formulation can be written as

$$AJ_2' + BJ_1^2 = Y^2 = \delta Y_0^2 \quad (1)$$

where A , B , δ are yield criterion parameters and are functions of fractional theoretical density, J_1 is the first invariant of the stress tensor, J_2' is the second invariant of the stress deviator and Y_0 and Y are yield strength of a solid and partially dense material having fractional theoretical density ρ , respectively [16]. The parameters J_1 and J_2' in the cylindrical coordinate system where the axis represents radial, circular and axial direction can be expressed as follows

$$J_2' = \frac{1}{6} [(\sigma_r - \sigma_\theta)^2 + (\sigma_\theta - \sigma_z)^2 + (\sigma_z - \sigma_r)^2] \quad (2)$$

$$J_1 = \sigma_r + \sigma_\theta + \sigma_z \quad (3)$$

Here for axisymmetric forging, $\sigma_r = \sigma_\theta$, J_2' and J_1^2 can be written as

$$J_2' = \frac{1}{6} (2\sigma_\theta^2 + 2\sigma_z^2 - 4\sigma_\theta\sigma_z) \quad (4)$$

$$J_1^2 = 4\sigma_\theta^2 + \sigma_z^2 + 4\sigma_\theta\sigma_z \quad (5)$$

Substituting Eq. (4) and Eq. (5) into Eq. (1) gives

$$\frac{A}{6} (2\sigma_\theta^2 + 2\sigma_z^2 - 4\sigma_\theta\sigma_z) + B(4\sigma_\theta^2 + \sigma_z^2 + 4\sigma_\theta\sigma_z) = \delta Y_0^2 \quad (6)$$

L. Hua et al. [4] has investigated and presented the values for yield criterion parameters based on plastic Poisson's ratio, relative density and flow stress of the matrix material and several yield criterion for sintered powder material were also compared with each other. The following yield criteria parameters are chosen in this

research as $A = 2 + \rho^2$, $B = (1 - \rho^2)/3$, $\delta = [(\rho - \rho_0)/(1 - \rho_0)]^2$. Eq. (6) now can be written as

$$Y_0 = \sigma_{eff} = \left[\frac{(1 - \rho_0)^2 (\sigma_z^2 - 2\sigma_\theta^2 - \rho(\sigma_\theta^2 - 2\sigma_\theta\sigma_z))}{(\rho - \rho_0)^2} \right]^{0.5} \quad (7)$$

Eq. (7) gives the expression for effective stress in terms of cylindrical coordinates.

According to Narayansamy et al. [17], the hoop stress (σ_θ) under triaxial stress state condition can be determined as given below:

$$\sigma_\theta = \left[\frac{2\alpha + \rho^2}{2 - \rho^2 + 2\rho^2\alpha} \right] \sigma_z \quad (8)$$

$$\text{where, } \alpha = \frac{d\varepsilon_\theta}{d\varepsilon_z}$$

The stress formability factor [10] is given as

$$\beta = \frac{J_1}{(3J_2')^{0.5}} = \frac{3\sigma_m}{\sigma_{eff}}, \quad (9)$$

$$\text{where, } \sigma_m = \frac{\sigma_r + \sigma_\theta + \sigma_z}{3} = \frac{2\sigma_\theta + \sigma_z}{3}, \text{ is the hydrostatic stress.}$$

The stress formability factor as expressed in Eq. (9) is used to describe the effect of mean stress and the effective stress on the forming limit of P/M compacts in upsetting.

4. Results and discussion

4.1 Densification

During the deformation process, such as the one carried out during this research, it is well established [6-9,17] that densification is continuously enhanced; therefore, densification is a function of induced strain. In this view, the relationship between fractional theoretical density and induced height strain during cold upsetting is

studied. A plot has been presented as shown in Fig. 1 between true height strain and percentage fractional theoretical density for Fe-0.35%C steel preforms for two different initial aspect ratios, namely, 0.40 and 0.60, these plots being drawn for two different lubricants namely no/nil and graphite lubricant conditions. The general observations of curves show that with the increasing height strain, densification is also continuously increasing irrespective of initial aspect ratio and lubricant condition. It is noted that the densification is higher during the initial stages of deformation with reduced height strain. During the initial stages of deformation large number of pores are present, thus bigger pores collapse and close with little enhancement in true height strain. The second stage follows steady state response indicating the pore closing rate has decreased with enhancement in axial deformation and at the final stage very little increase in densification is achieved. This is because during the final stages of deformation the cylindrical pores whose axis is aligned in the direction of pressing acts as stress risers and are difficult to deform and collapse hence very little enhancement in density is achieved. This behaviour is true irrespective of the initial aspect ratio and frictional constraints. Further, it is found that 0.40 aspect ratio preforms densification values are improved for any true height strain value when compared to the 0.6 aspect ratio provided the preforms initial theoretical density are same, however the final densification achieved before crack initiation on the free surface of the preforms is marginally different. The pore closure mechanism is faster in lower aspect ratio preform due to the lower pore bed height in comparison to higher aspect ratio preform and hence densification increases for lower aspect ratio preform.

The careful examination of Fig. 1 reveal that the densification rate of preform of aspect ratio of 0.4 is significantly higher for the graphite lubricant condition from the

start of the deformation process when compared to preform of aspect ratio of 0.6 however, during nil/no lubricant condition this phenomenon is only evident after mechanism 1. However, at the final stages of deformation the difference in densification achieved is small. This proves the fact that lower initial aspect ratio preform has better densification compared to higher aspect ratio preform for a given height strain level irrespective of the lubricant conditions.

Further it is found that nil/no lubricant condition (Fig. 1) exhibits higher densification rate right from the start of deformation (84% theoretical) to around 96% theoretical density when compared to the graphite lubricant condition. Thereafter, irrespective of the aspect ratio and lubricants employed, the achieved density is almost equal. A possible technical reason is that friction at die contact surfaces provides resistance to lateral deformation, which reinforces the vertical forming pressure and thus increases the densification of the material. This frictional condition during cold deformation in the lateral direction induces barreling in the preform which is the root cause of evolving the crack at free surface of the preform. Further, the deformation under graphite lubricant condition increases the height strain to fracture for both aspect ratios, hence the intensity of barreling increases with increasing frictional constraints. Also it is seen from Fig. 1 that the higher aspect ratio facilitates an increase in height strain to fracture irrespective of lubricant employed during cold deformation.

Figure 1: Influence of aspect ratios on the densification of iron-0.35% carbon sintered alloy powder preform during cold deformation under nil/no & graphite lubricants.

Cold working is one of the methods to promote strength in metals; in this case strain induced will be the prominent factor for a fully dense material. The same is true for P/M material too, however the additional factor that governs is pore closure or density attained. It is well established [18] that attaining full density besides the mode by which it is attained is the significant phenomenon that governs strength of P/M material. Thus a plot constructed for flow stress against attained density for Fe-0.35%C steel preforms during cold deformation under the influence of preforms geometries and lubricating conditions and is shown in Figure 2. It is seen that three different stages exist for flow stress against densification plot. There is little rise in stress values during the initial stage from its initial density (84% theoretical) to 87-88% theoretical density as the initial application of axial load is not sufficient to deform the preform. As the pores close (due to continued application of load) in the P/M preform higher levels of densification is achieved and the strength of the material is enhanced which in turn increases the stress values. The slope of the curve during the intermediate stage is lower than that of the initial stage due to the lateral deformation being pronounced after 88% theoretical density. However, the reason for an increase in flow stress values with little densification during the final stages of deformation is that the material is expected to strain harden. Further, it is observed for any value of percent fractional theoretical density, the lower aspect ratio preform deformed under nil/no lubricant condition experience higher stress values compared to higher aspect ratio preform. Further, the effect of frictional constraints is only evident during the final stages of deformation.

Figure 2: Influence of aspect ratios and lubricants on the relationship between the flow stress and percent fractional theoretical density of iron-0.35% carbon sintered alloy powder preform during cold deformation.

4.2 Poisson's ratio

During cold upsetting of powder metallurgy parts a substantial material flow occurs in lateral direction as well as axial direction due to the presence of voids. Poisson's ratio is defined as ratio between the lateral strain and axial strain and during the plastic deformation of conventional material the Poisson's ratio is equal to 0.5 to retain the volume constancy, however, this is not the case in powder metallurgy materials. Figure 3 has been drawn to demonstrate the relationship that exists between true diameter strain and true height strain. The initial aspect ratio is kept constant. It can be noted that the dashed line representing the relationship between diameter strain and height strain for a fully dense material and the curves for porous material are below the dashed line. Further, it can be seen that for a given height strain the diameter strain is more for graphite employed lubricant compared to nil/no lubricant condition indicating lateral deformation is pronounced in the case of graphite lubricated preform. In powder preform forging the present pores collapse and close reducing the volume hence, during the plastic deformation of P/M material the rate of change of diameter is less than that of a fully dense material resulting in Poisson's ratio values to be less than 0.5.

Figure 3: Relationship between true diameter strain and true height strain with the influence of lubricants of iron-0.35% carbon sintered alloy powder preform during cold deformation.

Further, a plot has been constructed to show the relationship between Poisson's ratio and percent fractional theoretical density achieved during powder preform forging of sintered iron-0.35% carbon alloy powder preforms, these plots being drawn for two different lubricants keeping the initial theoretical density and aspect ratio constant as shown in Figure 4. The characteristics nature of these curves follows three distinct stages. During the initial stages of deformation the Poisson's ratio values increases rapidly with little densification irrespective of the lubricants used. The intermediate stage of densification is treated as a steady state condition, where most of the densification occurs with very gradual increase in Poisson's ratio and during the final stages of deformation a rapid increase in Poisson's ratio occurred without much enhancement in densification. Further, it exhibits the tendency to approach a limiting value of 0.5. Further observation reveals that for a given percent theoretical density the Poisson's ratio value are higher for graphite lubricant condition compared to the nil/no lubricant condition as the lateral deformation is enhanced in the case of graphite lubricant. It can be concluded that graphite employed lubricant has enhanced the deformation when compared to the nil/no lubricant condition during cold upset forging.

Figure 4: Variation of Poisson's ratio with percent fractional theoretical density of iron-0.35% carbon sintered alloy powder preforms with different lubricants.

4.3 Micrograph analysis

Further, to understand the deformation behaviour of Fe-0.35%C the microstructure view of 1000X magnification is shown in Fig. 5(a), 5(b), 6(a) and 6(b) respectively.

Particularly, the view was selected one at the centre and other one at the extreme diametric side of each of the preforms in order to view the presence of porosities. The presence of porosity at the centre (refer Fig, 5(a) and 6(a)) was very little in comparison to extreme diametric view (refer Fig, 5(b) and 6(b)). Further, the pores present at the centre have round shape whilst the pores at extreme diametric side are elongated in the direction of metal flow. It can be said that effective closure of pores of a cylindrical preform at the centre is much higher in comparison to extreme diametric side. The effective closure of pores diminishes laterally outwards.

Figure 5(a) and 5(b): Microstructure view at centre and diametric extreme of the preform deformed under dry friction conditions respectively

Figure 6(a) and 6(b): Microstructure view at centre and diametric extreme of the preform deformed under graphite employed friction conditions respectively

4.4 Forming limit

In powder preform forging the upsetting operation is terminated or the repressing process is employed once the crack appears on the free surface to produce defect free parts [9]. Hence, the forming limit of powder metallurgy materials has significant implications in design of the preform geometry as well as dies. Figure 7 demonstrate the relationship between the height strain at fracture and initial aspect ratio. This figure also shows the effect of the lubricant on the aforesaid relationship. It can be seen from Figure 7 that an increase in initial aspect ratio from 0.4 to 0.6 increases the true height strain at fracture irrespective of the lubricant employed, however, the true height strain to fracture values are enhanced in the case of graphite lubricant condition compared to the nil/no lubricant condition. It can be concluded that increasing the

initial aspect ratio and reducing frictional constraints promotes height strain to fracture.

Figure 7: Relationship between height strain at fracture in cold deformation of iron-0.35% carbon sintered alloy powder preform with initial aspect ratios.

The relationship between true diameter strain at fracture and true height strain at fracture is shown in Figure 8. It is noted that under the application of graphite lubricant condition both true diameter strain at fracture and true height strain at fracture is enhanced for a given initial aspect ratio when compared to nil/no lubricant condition. Further, it is noted that the slope of the curve in the case of graphite lubricant condition is higher for true diameter strain at fracture against true height strain at fracture. Hence, it can be said that an increase of aspect ratio in graphite employed lubricant promotes substantial lateral deformation when compared to nil/no lubricant condition. However, this substantial lateral deformation only elongates the voids but not effectively closes; this is the reason graphite lubricant employed preforms not effectively promoted densification at the intermediate stages nevertheless before fracture the maximum density attained is in par with nil/no lubricant employed preforms (refer Fig 1). These plots are essential in designing of preform geometries and dies for cold upsetting operations.

Figure 8: Relationship between true diameter strain and true height strain at fracture in cold deformation of iron-0.35% carbon sintered alloy powder preform with the influence of initial aspect ratio and frictional condition.

4.5 Formability stress index

Formability is a measure of the extent of deformation that a material can withstand the induced internal stresses of forming prior to fracture occurred [17]. It has been reported [10] that the effect of relative density (fractional theoretical density) is a major concern on formability of P/M material. It is imperative to note that the extent to which P/M material are formed as well as maximum density been achieved are the major concerns for structural applications. Therefore formability stress index as a function of fractional theoretical density and strain induced is constructed and shown in Fig. 9 and Fig. 10 respectively. These curves are plotted for two initial aspect ratios for two different frictional constraints. From Fig. 9 it is seen as the densification increases, the formability stress index increase and as the relative density approaches 1.0, there is significant increase in the formability stress index due to the closing of pores during densification or plastic deformation. The characteristics nature of the curve is similar irrespective of the aspect ratio and lubricant employed.

Figure 9: Relationship between formability stress index and fractional theoretical density of iron-0.35% carbon sintered alloy powder preform with the influence of initial aspect ratio and frictional condition.

From Fig. 10 for all aspect ratio and frictional constraints, the axial strain increases with increasing values of formability stress index. For equal height strain level, the lower aspect ratio preform exhibits improved formability stress index compared to that of larger aspect ratio irrespective of the lubricant employed. Further interesting

point to note is that increasing the aspect ratio and decreasing the friction conditions are obviously increasing the deformation, however the maximum formability stress index value attained by the Fe-0.35%C preforms are almost same irrespective of variables considered in this investigation but at various strain values.

Figure 10: Relationship between formability stress index and true height strain of iron-0.35% carbon sintered alloy powder preform with the influence of initial aspect ratio and frictional condition.

5. Conclusions

The preform geometry and frictional constraints during cold upsetting operations affects the densification behaviour, the forming limit and the formability characteristics of Fe-0.35%C P/M steels. Accordingly the major conclusions have been drawn that are as follows.

- The amount of densification is found to be high when decreasing aspect ratio and increasing friction conditions, however the final achievements of densification were almost same irrespective of the variables used in the investigation. Further Poisson's ratio showed a tendency to a limiting value of 0.5 as densification progresses towards the vicinity of near theoretical density.
- Fracture strains include height and diameter strain found to increase substantially when friction condition decreases but it is not for granted to promote densification, the similar phenomena is true when aspect ratio increased, however the effect is mild.

- Formability stress index was computed and its behavior against promoted densification with respect to the considered variables is literally negligible, however against strain induced is prominent.
- The porosity presented at the centre are small in amount and round in shape while at the extreme diametric side more porosities are seen and it is elongated in the direction of metal flow which in turn will appear as visible crack at the free surface.

Acknowledgement

The authors are highly indebted to M/s Asbury Graphite Mills, USA, for their kind gesture in providing graphite powders for the present research work.

References

- [1] Poshal G, Ganesan P. Neural network approach for the selection of processing parameters of aluminium-iron composite preforms during cold upsetting. *J Eng Manufact* 2009;224:459-72.
- [2] Rosochowski A, Beltrando L, Navarro S. Modeling of density and dimensional changes in re-pressing/sizing of sintered components. *J Mater Process Technol* 1998;80:188-94.
- [3] Lindsog P. Economy in car-making – powder metallurgy, Global Automotive Manufacturing and Technology, Technology & Services, Business Briefing. London: UK; 2003.
- [4] Hua L, Qin X, Mao H, Zhao Y. Plastic deformation and yield criterion for compressible sintered powder materials. *J Mater Process Technol* 2006;180:174-8.

- [5] Liu Y, Chen LF, Tang HP, Liu CT, Liu B, Huang BY. Design of powder metallurgy titanium alloys and composites. *Mater Sci Eng A* 2006;418:25-35.
- [6] Narayanasamy R, Selvakumar N. Deformation behaviour of cold upset forming of sintered Al-Fe composite preforms. *J Eng Mater Technol* 2005;127:251-6.
- [7] Rajeshkannan A, Pandey KS, Shanmugam S, Narayanasamy R. Sintered Fe-0.8%C-1.0%Si-0.4%Cu P/M preform behaviour during cold upsetting. *J Iron Steel Res Int* 2008;15:92-7.
- [8] Kuhn HA, Lawley A. Powder metallurgy processing. New York: Academic press; 1978. p. 99-138.
- [9] Rajeshkannan A, Pandey KS, Shanmugam S. Some investigation on the cold deformation behaviour of sintered iron-0.8% carbon alloy powder preforms. *J Mater Process Technol* 2008;203:542-7.
- [10] Rahman MA, El-Sheikh MN. Workability in forging of powder metallurgy compacts. *J Mater Process Technol* 1995;54:97-102.
- [11] Simchi A. Effects of lubrication procedure on the consolidation, sintering and microstructural features of powder compacts. *Mater Des* 2003;24:585-94.
- [12] Zhang XQ, Peng YH, Li MQ, Wu SC, Ruan XY. Study of workability limits of porous materials under different upsetting conditions by compressible rigid plastic finite element method. *J Mater Eng Perform* 2009;9:164-9.
- [13] Ramesh B, Senthivelan T. Formability characteristics of aluminium based composite-a review. *Int J Eng Technol* 2010;2:1-6.

- [14] Lee SR, Lee YK, Park CH, Yang DY. A new method of preform design in hot forging by using electric field theory. *Int J Mech Sci* 2002;44:773-92.
- [15] Butuc MC, Gracio JJ, Rocha BA. An experimental and theoretical analysis on the application of stress-based forming limit criterion. *Int J Mech Sci* 2006;48:414-29.
- [16] Lewis RW, Khoei AR. A plasticity model for metal powder forming processes. *Int J Plast* 2001;17:1659-92.
- [17] Narayanasamy R, Ramesh T, Pandey KS. Some aspects on workability of aluminium-iron powder metallurgy composite during cold upsetting. *Mater Sci Eng A* 2005;391:418-26.
- [18] Rajeshkannan A, Narayan S. Strain hardening behaviour in sintered Fe-0.8%C-1.0%Si-0.8%Cu powder metallurgy preform during cold upsetting. *J Eng Manufact* 2009;223:1567-74.

List of Figures

Figure 1: Influence of aspect ratios on the densification of iron-0.35% carbon sintered alloy powder preform during cold deformation under nil/no & graphite lubricants.

Figure 2: Influence of aspect ratios and lubricants on the relationship between the flow stress and percent fractional theoretical density of iron-0.35% carbon sintered alloy powder preform during cold deformation.

Figure 3: Relationship between true diameter strain and true height strain with the influence of lubricants of iron-0.35% carbon sintered alloy powder preform during cold deformation.

Figure 4: Variation of Poisson's ratio with percent fractional theoretical density of iron-0.35% carbon sintered alloy powder preforms with different lubricants.

Figure 5(a) and 5(b): Microstructure view at centre and diametric extreme of the preform deformed under dry friction conditions respectively.

Figure 6(a) and 6(b): Microstructure view at centre and diametric extreme of the preform deformed under graphite employed friction conditions respectively.

Figure 7: Relationship between height strain at fracture in cold deformation of iron-0.35% carbon sintered alloy powder preform with initial aspect ratios.

Figure 8: Relationship between true diameter strain and true height strain at fracture in cold deformation of iron-0.35% carbon sintered alloy powder preform with the influence of initial aspect ratio and frictional condition.

Figure 9: Relationship between formability stress index and fractional theoretical density of iron-0.35% carbon sintered alloy powder preform with the influence of initial aspect ratio and frictional condition.

Figure 10: Relationship between formability stress index and true height strain of iron-0.35% carbon sintered alloy powder preform with the influence of initial aspect ratio and frictional condition.

List of Table

Table 1: Characterization of iron powder and Fe-0.35%C blend.

Table 2: Sieve size analysis of iron powder.

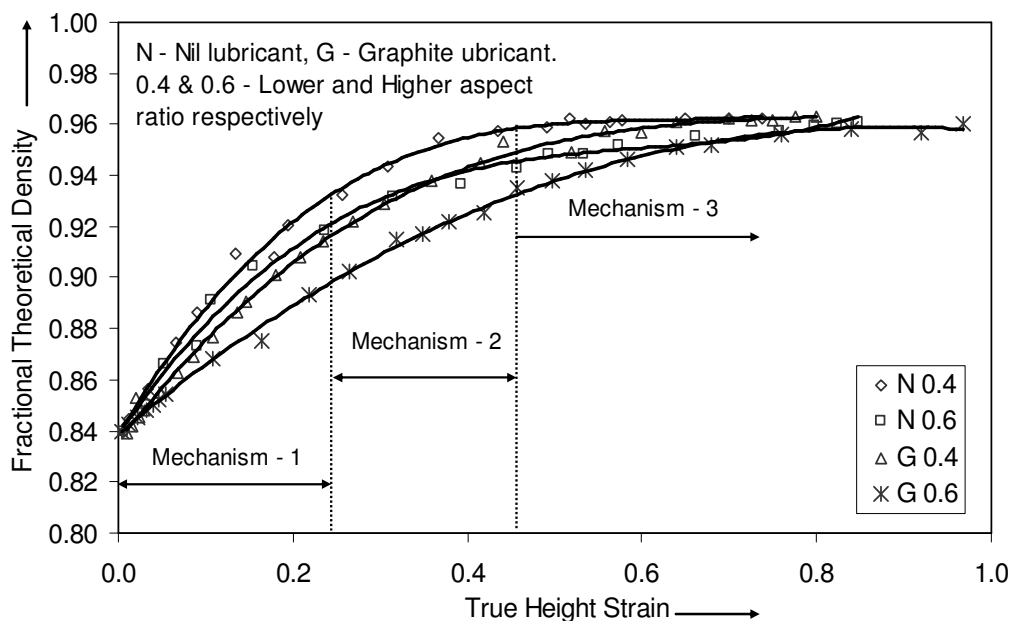


Figure 1: Influence of aspect ratios on the densification of iron-0.35% carbon sintered alloy powder preform during cold deformation under nil/no & graphite lubricants.

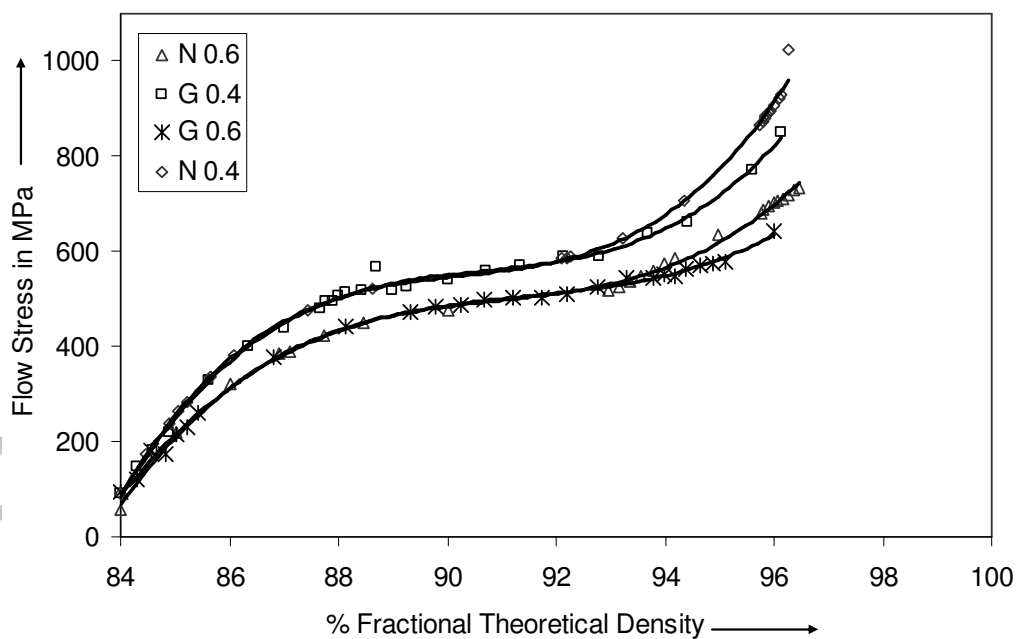


Figure 2: Influence of aspect ratios and lubricants on the relationship between the flow stress and percent fractional theoretical density of iron-0.35% carbon sintered alloy powder preform during cold deformation.

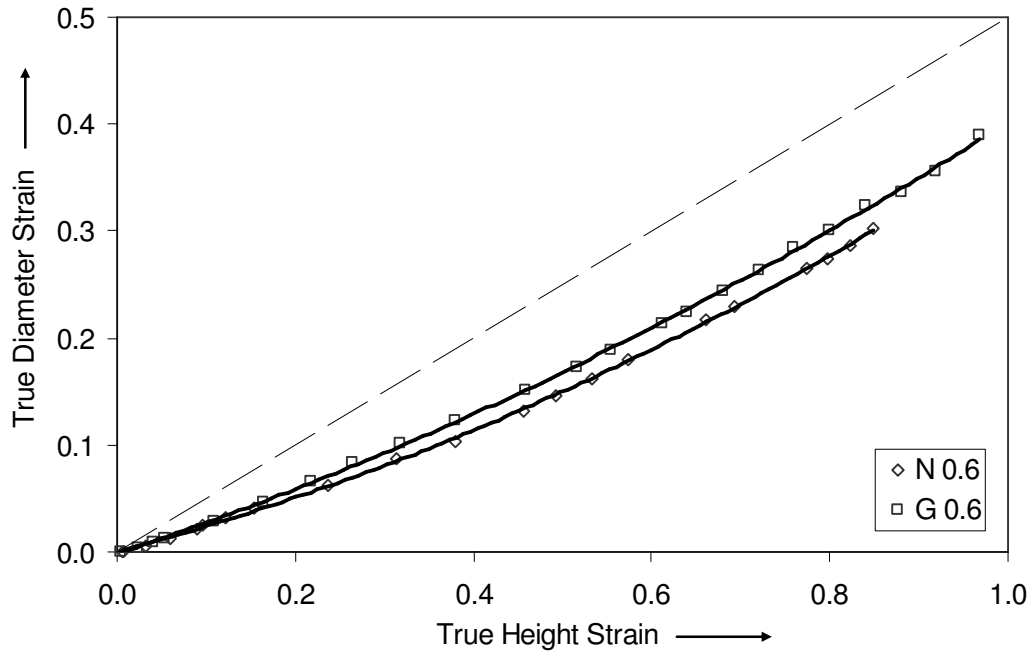


Figure 3: Relationship between true diameter strain and true height strain with the influence of lubricants of iron-0.35% carbon sintered alloy powder preform during cold deformation.

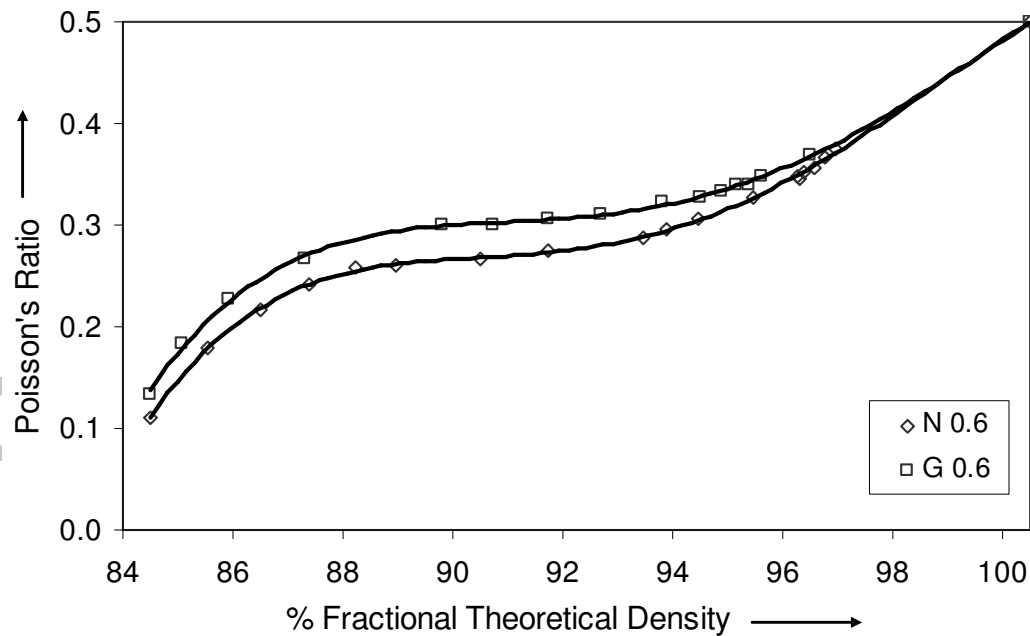


Figure 4: Variation of Poisson's ratio with percent fractional theoretical density of iron-0.35% carbon sintered alloy powder preforms with different lubricants.

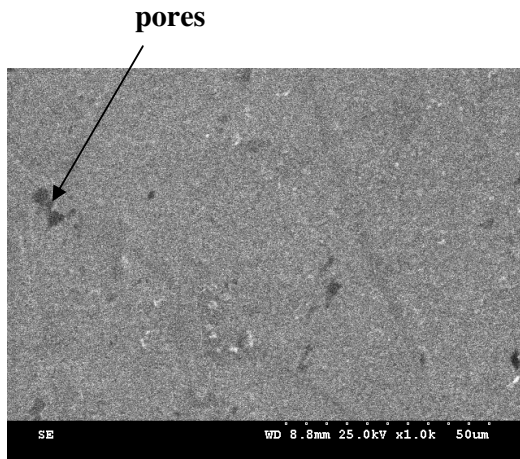


Figure 5(a)

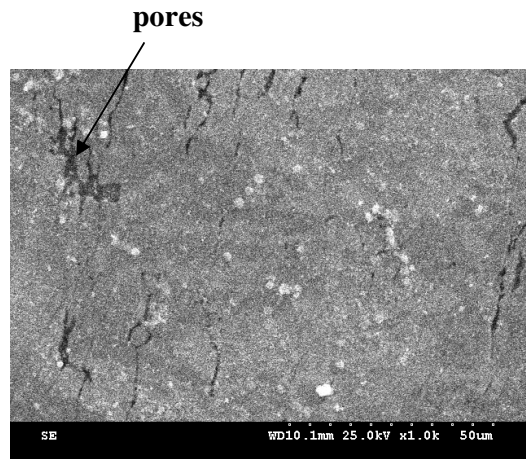


Figure 5(b)

Figure 5(a) and 5(b): Microstructure view at centre and diametric extreme of the preform deformed under dry friction conditions respectively

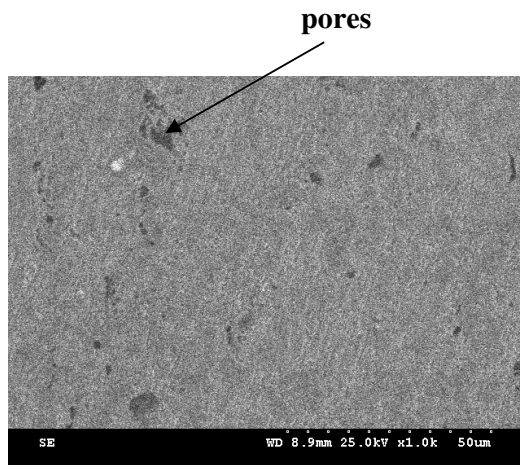


Figure 6(a)

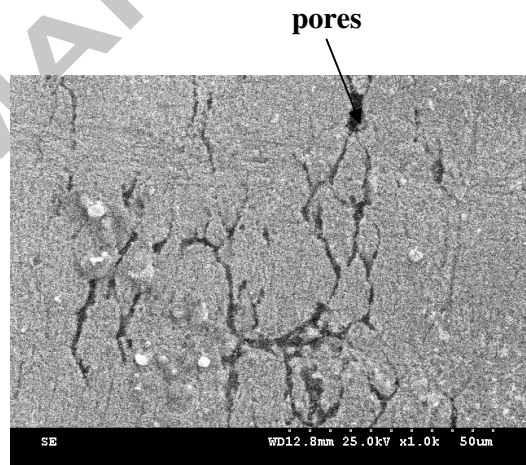


Figure 6(b)

Figure 6(a) and 6(b): Microstructure view at centre and diametric extreme of the preform deformed under graphite employed friction conditions respectively

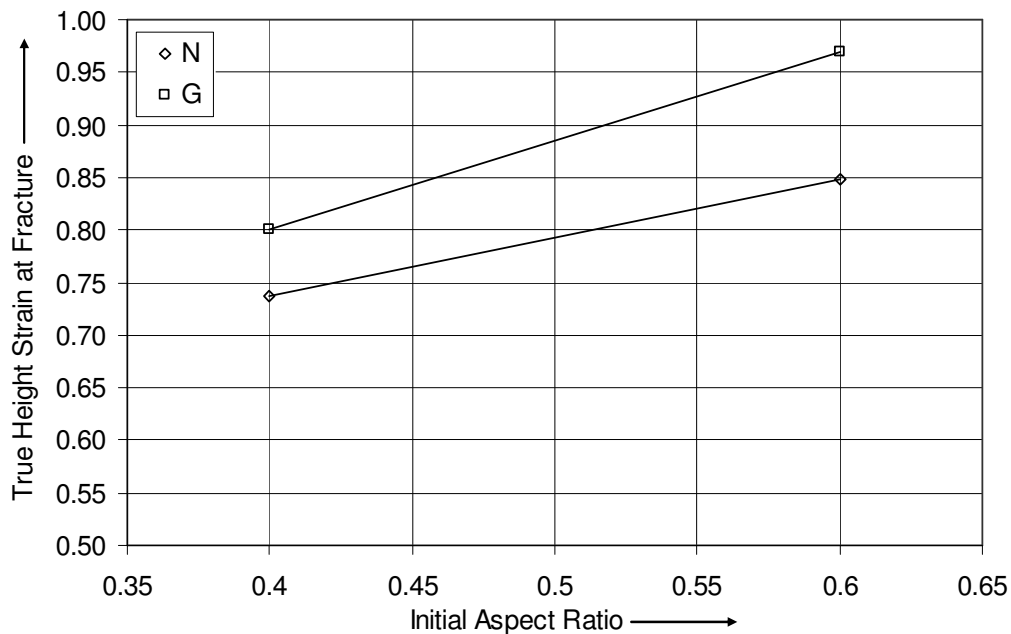


Figure 7: Relationship between height strain at fracture in cold deformation of iron-0.35% carbon sintered alloy powder preform with initial aspect ratios.

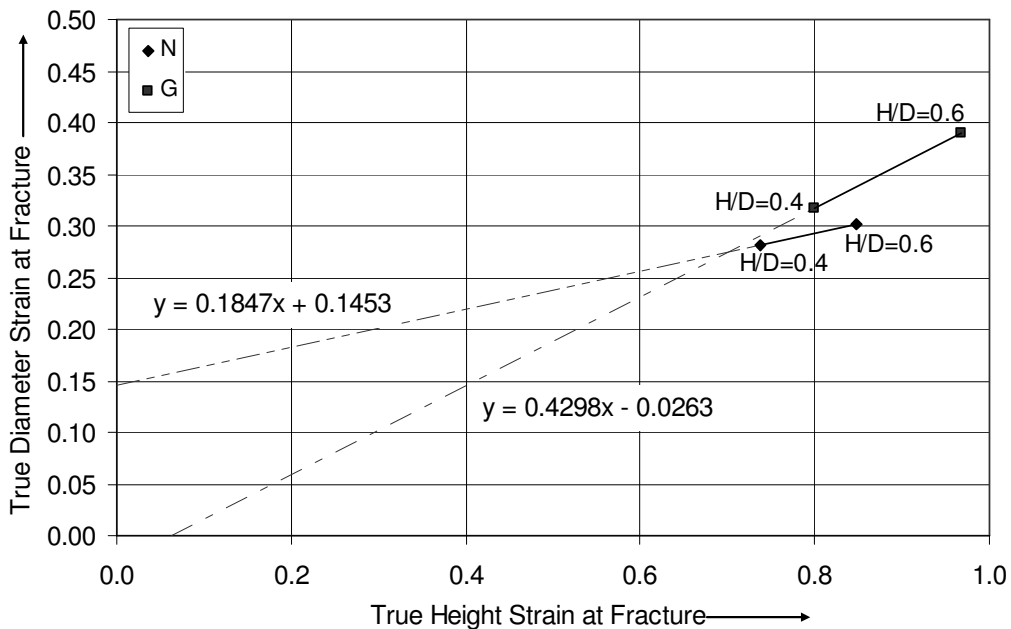


Figure 8: Relationship between true diameter strain and true height strain at fracture in cold deformation of iron-0.35% carbon sintered alloy powder preform with the influence of initial aspect ratio and frictional condition.

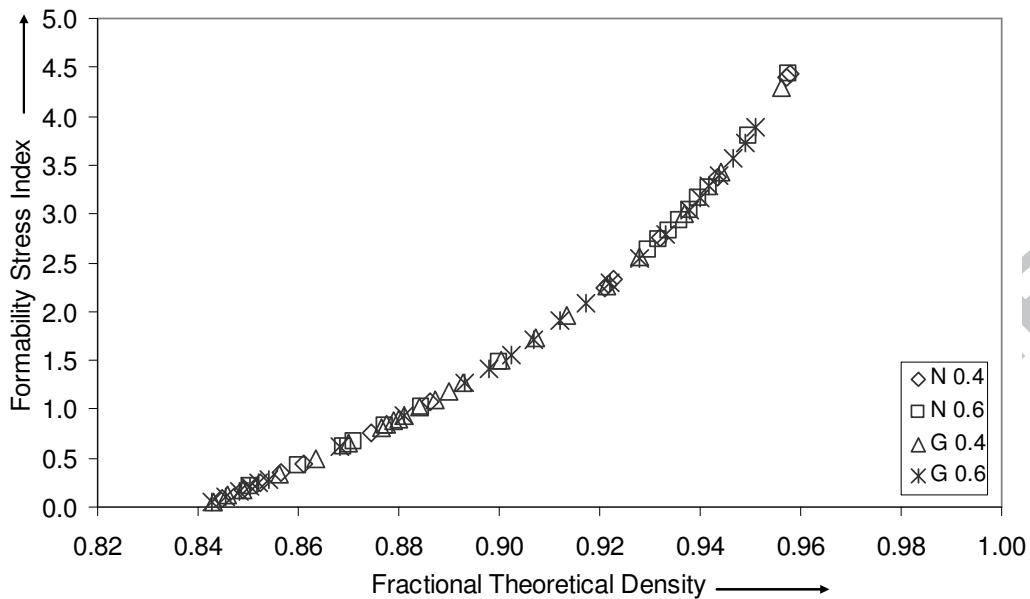


Figure 9: Relationship between formability stress index and fractional theoretical density of iron-0.35% carbon sintered alloy powder preform with the influence of initial aspect ratio and frictional condition.

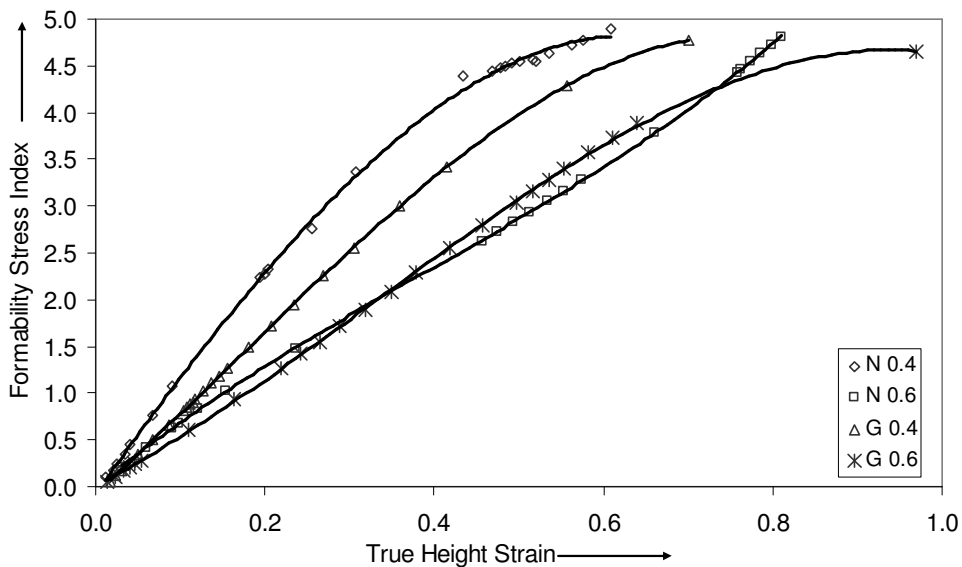


Figure 10: Relationship between formability stress index and true height strain of iron-0.35% carbon sintered alloy powder preform with the influence of initial aspect ratio and frictional condition.

Table 1. Characterization of iron powder and Fe-0.35%C blend

Si. No.	Property	Iron	Fe-0.35%C Blend
1.	Apparent Density (g/cc)	3.38	3.37
2.	Flow rate, (s/50g) by Hall Flow Meter	26.3	28.1
3.	Compressibility (g/cc) at pressure of 430±10MPa	6.46	6.26

Table 2. Sieve size analysis of iron powder

Sieve size (μm)	150	+125	+100	+75	+63	+45	-45
Wt % Ret.	10.60	24.54	15.46	19.90	11.10	8.40	10.00